

Microscopic origin of level attraction for a coupled magnon-photon system in a microwave cavity

Igor Proskurin^{1,2}, Rair Macêdo³, Robert L Stamps¹

¹ Department of Physics and Astronomy, University of Manitoba, Winnipeg, Manitoba R3T 2N2, Canada

² Institute of Natural Sciences and Mathematics, Ural Federal University, Ekaterinburg 620002, Russia

³ James Watt School of Engineering, Electronics & Nanoscale Engineering Division, University of Glasgow, Glasgow G12 8QQ, UK

E-mail: Igor.Proskurin@umanitoba.ca

Abstract. We discuss various microscopic mechanisms for level attraction in a hybridized magnon-photon system of a ferromagnet in a microwave cavity. The discussion is based upon the electromagnetic theory of continuous media where the effects of the internal magnetization dynamics of the ferromagnet are described using dynamical response functions. This approach is in agreement with quantized multi-oscillator models of coupled photon-magnon dynamics. We demonstrate that to provide the attractive interaction between the modes, the effective response functions should be diamagnetic. Magneto-optical coupling is found to be one mechanism for the effective diamagnetic response, which is proportional to photon number. A dual mechanism based on the Aharonov-Casher effect is also highlighted, which is instead dependent on magnon number.

Keywords: level attraction, microwave cavities, magneto-optical interactions, cavity optomagnonics

1. Introduction: mode attraction in microwave cavities

Microwave cavity resonators are useful for coupling microwave photons to various excitations including mechanical [1], acoustic [2], and magnetic degrees of freedom [3]. In magnetism, hybridization between cavity modes and ferromagnetic resonances in the form of cavity magnon-polaritons has been demonstrated and studied in a number of systems [4, 5, 6, 7, 8, 9, 10, 11, 12]. Cavity optomagnonics was proposed recently with analogues to optomechanics [13, 14, 15, 16]. In optomagnonics, cavity photons couple to magnetic excitations via the magneto-optical interactions, which allows characterization using a well-established optomechanical Hamiltonian [15, 16], and, as a consequence, one should be able to observe optomechanical effects in magnetic systems [17]. Various phenomena have been proposed for coupled magnon-photon systems inside microwave cavities including Brillouin-scattering-induced transparency

in whispering gallery resonators [18, 19, 20], collective dynamics of spin textures [21, 22], and photon-mediated nonlocal interactions [23, 24, 25, 26].

Recently, for certain positions of a magnetic sample a mode attraction regime has been observed within a cylindrical [27] or a planar cavity [28]. Mode attraction is a general feature known already to be possible in dynamic optomechanical systems [29]. Naturally, it requires a certain instability mechanism being provided, which in optomechanical context is realized via the negative frequency in the effective Hamiltonian of a driven system [29]. In contrast to usual mode hybridization, mode attraction is characterized by a region where the real parts of the eigenfrequencies coalesce marked by the exceptional points where the eigenmodes collapse [30, 31]. In Ref. [27], the level attraction for cavity magnon-polaritons was interpreted as a manifestation of Lenz's law in a phenomenological electrical circuit model. The mechanism for level attraction between strongly interacting spin-photon excitations was also proposed for a system with two driving terms with a phase offset [32], which was recently realized in a re-entrant cavity resonator using two separate drives [33, 34].

The purpose of this paper is to discuss possible microscopic material mechanisms for mode attraction in ferromagnetic systems. Most of these mechanisms can be thought of in terms of an effective diamagnetic response of the system. To show this, we will use the approach based on the Maxwell's equations in dispersive media, where the internal magnetization dynamics is taken into account through response functions and constitutive relations [35].

Before going to specific details, we illustrate the essential ideas with a three coupled oscillator model. Such a model is obtained if we take a small magnetic specimen with the magnetization $\mathbf{M}(t)$ in a static magnetic field \mathbf{H}_0 interacting with the microwave field $\mathbf{h}(t)$ of the cavity, as schematically shown in Fig. 1 (a). This model shows the level attraction in the unstable regime where the magnetization is opposite to the magnetic field, which formally corresponds to a negative magnon frequency. Such configuration is, of course, unphysical. However, it illustrates a general rule that the mode attraction is related to an instability in the system. In the linear approximation for magnetization dynamics, the total interacting Hamiltonian can be written as (see Appendix A for details)

$$\mathcal{H} = \hbar\omega_c \left(a_L^\dagger a_L + a_R^\dagger a_R \right) + \hbar\Omega_m b^\dagger b + \hbar g_0 \left[(a_R + a_L^\dagger) b + \text{H.c.} \right] + \mathcal{H}_{\text{drv}}, \quad (1)$$

where a^\dagger (a) is the creation (annihilation) operator for two degenerated cavity photon modes with right (R) and left (L) polarizations and the frequency ω_c , b and b^\dagger describe the magnon oscillator with the frequency Ω_m , g_0 denotes the magnon-photon coupling parameter, and the last term is the external driving energy at the frequency ω , $\mathcal{H}_{\text{drv}} = i\hbar\sqrt{\kappa_{\text{ex}}}\left[\alpha_{\text{in}}a_R \exp(-i\omega t) - \alpha_{\text{in}}^*a_R^\dagger \exp(i\omega t)\right]$ with the amplitude α_{in} and coupling parameter κ_{ex} .

The qualitative behavior of this model can be understood directly from the Hamiltonian (1). For $\Omega_m \approx \omega_c$, the dominant contribution comes from the interaction term proportional to $a_L^\dagger b + a_L b^\dagger$ that describes a hybridization between the left polarized

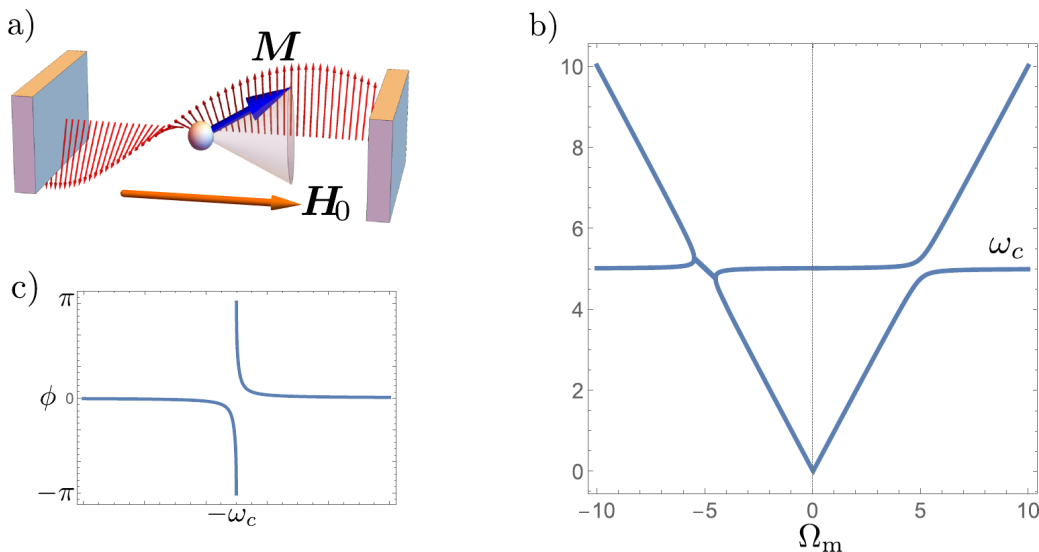


Figure 1. a) Schematic picture of a small ferromagnetic sample interacting with circularly polarized electromagnetic wave inside a microwave cavity. b) Energy dispersion for the Hamiltonian (1) as a function of Ω_m showing level repulsion near ω_c and level attraction at $-\omega_c$. c) Phase shift in the equation (2) as a function of ω demonstrating 2π jump near $-\omega_c$.

electromagnetic wave and the magnon mode precessing in the same direction, while a_R remains decoupled [36]. More interesting behavior takes place for $\Omega_m \approx -\omega_c$, where the term $a_R b + a_R^\dagger b^\dagger$ is dominant, which is known as the ‘two-mode squeezing’ regime in optomechanics [1]. In this case, the level attraction regime is observed between the magnon and the right-polarized cavity mode in the region $(\Omega_m + \omega_c)^2 < 4g^2$ [29]. The whole picture is summarized in Fig. 1 (b).

Another salient feature in the mode attraction regime of the three oscillator model appears with varying the frequency of the drive around the point $\omega = -\omega_c$ when all three modes are degenerated, $\omega_c = \Omega_m$. This appears as a phase shift between the driving field α_{in} and the driven cavity mode a_R . If we introduce the dissipation in the magnon channel, $\Omega_m - i\kappa_m$, and neglect cavity dissipation, phase shift between the driving term and the response field is estimated as

$$\tan \phi = \frac{\kappa_m(\omega^2 - \omega_c^2)}{(\omega^2 - \omega_c^2)(\omega + \Omega_m) + 2g_0^2\omega_c}, \quad (2)$$

which contains contributions from two degenerated cavity modes with different polarizations and the magnon mode. When all modes are degenerated, $\Omega_m = -\omega_c$, these two contributions provide the phase shifts of $+\pi$ and $-\pi$ around $\omega = -\omega_c$ that results in a characteristic 2π phase jump as shown in Fig. 1 (c). We believe that similar mechanism may be behind the phase shift reported in Ref. [27]. We note, however, that within this illustration, 2π phase shift occurs at negative frequencies, whereas in the physical region $\omega \approx \omega_c$ it equals to π . Below, we will consider the response functions that can bring 2π phase jump to positive ω .

As already mentioned, the condition $\Omega_m \approx -\omega_c$ represents an unstable configuration

where \mathbf{M} and \mathbf{H}_0 are antiparallel. Another possible scenario would require fully dissipative imaginary coupling constant g_0 . Either possibility explains why level attraction was not observed previously for cavity magnon-polaritons. In this paper, we discuss physical mechanisms that are not fully dissipative, but instead arise from effective ‘diamagnetic’ responses where the reaction of the system is towards compensating the applied excitation. This can be somehow from the cavity itself, as proposed in Refs. [27, 28], or through some mechanism in the sample response. We consider here possible mechanisms first via the electromagnetic pressure on the sample through electro-optics, and second via the magnon pressure on the cavity through the Aharonov-Bohm mechanism.

In the following we construct a classical electromagnetic theory for the measured responses in terms of cavity and sample impedances. This allows us to define a tensor magnetic response for cavity-magnon coupling through either magnetic or electro-optical mechanisms. We demonstrate that magneto-optical coupling, or more specifically, the inverse Faraday effect, provides one possibility for the effective diamagnetic response, which being quantized, leads to a linearized optomagnonic Hamiltonian [15, 16]. Another possible scenario for the attractive regime comes from the Aharonov-Casher effect [37]. As we discuss at the end, this effect can be considered as dual to the magneto-optical coupling. In both scenarios, the magnon-photon interaction is driven by the cavity electric field.

2. Electromagnetic theory and diamagnetic response

A theory sufficiently complex to allow for different placements within a cavity in an actual experiment can be obtained using classical electrodynamics. This is most naturally formed in terms of impedances, and provides a direct connection to the scattering matrix element $S_{21}(\omega)$ typically measured in experiment. Frequency shifts and phase can be obtained from the complex scattering elements. These are obtained using standard classical electromagnetic theory in terms of energies W_e and W_m , defined over the sample volume V_S as

$$W_e = i\omega \int d^3r [\hat{\epsilon}(\omega) - \hat{\epsilon}_0] \mathbf{E} \cdot \mathbf{E}_0^*, \quad (3a)$$

$$W_m = i\omega \int d^3r [\hat{\mu}(\omega) - \hat{\mu}_0] \mathbf{H} \cdot \mathbf{H}_0^*, \quad (3b)$$

where the complex electric permittivity, $\hat{\epsilon} = 1 + \hat{\alpha}$, and magnetic permeability, $\hat{\mu} = 1 + \hat{\chi}$ are different from those for the free space due to the presence of the sample. The cavity electric and magnetic fields satisfy Maxwell’s equations in free space and are \mathbf{E}_0 and \mathbf{H}_0 . The fields perturbed by the sample are \mathbf{E} and \mathbf{H} . Together the energies provide the sample contribution to the measured impedance $Z_S = W_e - W_m$ [38, §6.10]. The perturbative impedance Z_S can then be simply added to a cavity impedance Z_c with parameters determined by unloaded measurements.

The required properties needed to construct Z_S from the response functions for the

loaded cavity can be understood in terms of the electromagnetic theory of continuous media. In this approach, we ignore at the beginning the finite sample size and describe the field inside the cavity by the Maxwell's equations

$$\nabla \times \mathbf{E} = -\partial_t (\mu_0 \hat{\mu} \mathbf{H}), \quad \nabla \cdot (\varepsilon_0 \hat{\varepsilon} \mathbf{E}) = 0, \quad (4a)$$

$$\nabla \times \mathbf{H} = \partial_t (\varepsilon_0 \hat{\varepsilon} \mathbf{E}), \quad \nabla \cdot (\mu_0 \hat{\mu} \mathbf{H}) = 0, \quad (4b)$$

By expanding the fields, $\mathbf{E} = \mathbf{E}_0 + \delta \mathbf{E}$ and $\mathbf{H} = \mathbf{H}_0 + \delta \mathbf{H}$, where $\delta \mathbf{E}$ and $\delta \mathbf{H}$ are related to the sample, we rewrite the equations above in the form

$$\nabla \times \delta \mathbf{E} + \partial_t (\mu_0 \hat{\mu} \delta \mathbf{H}) = -\partial_t (\mu_0 \hat{\chi} \mathbf{H}_0), \quad (5a)$$

$$\nabla \times \delta \mathbf{H} - \partial_t (\varepsilon_0 \hat{\varepsilon} \delta \mathbf{E}) = \partial_t (\varepsilon_0 \hat{\alpha} \mathbf{E}_0), \quad (5b)$$

where the free space cavity field can be considered as driving terms, which provide the response determined by the material functions of the medium.

Let us consider a situation where the plane electromagnetic wave is propagating in a homogeneous dispersive birefringent medium along the gyrotropic axis taken as z direction. In this case, we take magnetic susceptibility tensor in the form

$$\hat{\chi}(\omega) = \begin{pmatrix} \chi_1(\omega) & i\chi_2(\omega) & 0 \\ -i\chi_2(\omega) & \chi_1(\omega) & 0 \\ 0 & 0 & 0 \end{pmatrix}, \quad (6)$$

and $\hat{\varepsilon} = 1$ for simplicity. Transforming (5a) and (5b) to the ω -domain, and replacing ∂_z by $i\omega_c/c$, where ω_c is some characteristic frequency of the cavity, we obtain

$$\begin{pmatrix} \mu_0\omega(1 + \chi_1) & i\mu_0\omega\chi_2 & 0 & \omega_c/c \\ -i\mu_0\omega\chi_2 & \mu_0\omega(1 + \chi_1) & -\omega_c/c & 0 \\ 0 & -\omega_c/c & \varepsilon_0\omega & 0 \\ \omega_c/c & 0 & 0 & \varepsilon_0\omega \end{pmatrix} \begin{pmatrix} \delta H_x \\ \delta H_y \\ \delta E_x \\ \delta E_y \end{pmatrix} = -\mu_0\omega \begin{pmatrix} \hat{\chi}(\omega) \mathbf{H}_0 \\ 0 \end{pmatrix}. \quad (7)$$

If we include dissipation into account, χ_1 and χ_2 become complex. In this situation, the equation above has the exceptional points at the frequencies, which satisfy the relation $\chi_2(\omega) - \chi_1(\omega) = 2i\omega_c/\omega$, where the matrix on the left hand side does not have a diagonal form [31].

Calculating the circular components of the response magnetic field from equation (7), we obtain

$$\delta H^{(\pm)}(\omega) = -\frac{[\chi_1(\omega) \pm \chi_2(\omega)] \omega^2 \delta H_0^{(\pm)}}{[1 + \chi_1(\omega) \pm \chi_2(\omega)] \omega^2 - \omega_c^2}, \quad (8)$$

where $\delta H^{(\pm)} = \delta H_x \pm i\delta H_y$, which is directly related to the impedance of the loaded cavity via equations (3a, 3b). If we take the components of the susceptibility for the ferromagnetic resonance [36], $\chi_1(\omega) = \gamma M_s \Omega_m / (\Omega_m^2 - \omega^2)$ and $\chi_2(\omega) = \gamma M_s \omega / (\Omega_m^2 - \omega^2)$, we obtain a result consistent with equations (A.7)–(A.9)

$$\delta H^{(\pm)}(\omega) = -\frac{\gamma M_s \omega^2 \delta H_0^{(\pm)}}{(\omega^2 - \omega_c^2)(\Omega_m \mp \omega) + \gamma M_s \omega^2}, \quad (9)$$

which shows level repulsion behavior around $\omega \approx \Omega_m$. To obtain level attraction instead of repulsion, we formally need a ‘diamagnetic’ response here, which corresponds to $\gamma M_s < 0$.

2.1. Inverse Faraday effect mechanism

From the physical point of view, the effective resonant diamagnetic response may be realized if we consider nonlinear effects in light-matter interactions. One particular example is the inverse Faraday effect [39, §101], where circular polarized components of the electric field create an effective magnetic field $\mathbf{H}^{\text{eff}}(t) = i\varepsilon_0 f \mathbf{E}(t) \times \mathbf{E}^*(t)/4$, where $\mathbf{E}(t)$ is the electric field amplitude in the complex representation, $\mathbf{E} = (\mathbf{E} + \mathbf{E}^*)/2$, and f is the material dependent parameter. The effective magnetic field is able to drive the dynamics of the magnetization towards the resonance, which can be taken into account in Maxwell's equations through the modulation of the electric permittivity. Compared to the usual magneto-dipole coupling between the magnetization and the cavity magnetic field, we expect that this mechanism is dominant in the nodes of the cavity modes, where the magnetic field is small, while the electric field is maximal. By moving a small specimen inside the cavity, we can tune the relative strength of different coupling mechanisms, which changes the hybridization picture [27].

For illustration, we consider the experimental setup shown in Fig. 2 (a), where the cavity electromagnetic wave is excited along the x -direction perpendicular to the saturation axis of the magnetization, which is taken as z -axis. In this case, the displacement field generated by the inverse Faraday effect is given by $\delta D_i(t) = i\varepsilon_0 f \epsilon_{ijx} m_x(t) E_j(t)$, where ϵ_{ijk} denotes the Levi-Civita tensor. If we consider only linear terms in the fluctuating parts of the fields, and transform to the Fourier space, the effective response that takes into account resonant magnetization behavior can be estimated as

$$\begin{pmatrix} \delta \mathcal{D}_y(\omega) \\ \delta \mathcal{D}_z(\omega) \end{pmatrix} = -\frac{\varepsilon_0^2 f^2}{4} \chi_{xx}(\omega - \omega_L) \begin{pmatrix} |\mathcal{E}_{0z}|^2 & -\mathcal{E}_{0y}^* \mathcal{E}_{0z} \\ -\mathcal{E}_{0z}^* \mathcal{E}_{0y} & |\mathcal{E}_{0y}|^2 \end{pmatrix} \begin{pmatrix} \delta \mathcal{E}_y(\omega) \\ \delta \mathcal{E}_z(\omega) \end{pmatrix}, \quad (10)$$

where $\mathcal{D}(\omega) = [\mathcal{D}(\omega) + \mathcal{D}^*(\omega)]/2$, \mathcal{E}_0 and ω_L are the amplitude and the frequency of the driving field, and we neglected the terms with $\mathcal{E}(\omega \pm 2\omega_L)$. The details can be found in Appendix B. Equation (10) shows that in the linear approximation the inverse Faraday effect provides an effective dielectric resonant permittivity proportional to the intensity of the driving field and consistent with the macroscopic Lenz's effect. However, we note that such power dependence of the parameters has not been observed in recent experiments [27, 28], which means that these systems require a different microscopic explanation. We expect that the results of this section will be relevant to optomagnonic systems discussed in Refs. [15, 16].

If we apply the formalism of equations (5a, 5b) together with the effective permittivity in (10), excluding the magnetic field, we obtain the following equations for the fluctuating cavity electric field

$$\begin{pmatrix} \omega_c^2 - \omega^2 + |g_z|^2 \chi_{xx}(\bar{\Delta}) \omega^2 & -g_y^* g_z \chi_{xx}(\bar{\Delta}) \omega^2 \\ -g_y g_z^* \chi_{xx}(\bar{\Delta}) \omega^2 & \omega_c^2 - \omega^2 - \chi_{yy}(\omega) \omega^2 + |g_y|^2 \chi_{xx}(\bar{\Delta}) \omega^2 \end{pmatrix} \begin{pmatrix} \delta \mathcal{E}_y \\ \delta \mathcal{E}_z \end{pmatrix} = 0, \quad (11)$$

where we have introduced effective coupling constants $g_i = \varepsilon_0^{1/2} f \mathcal{E}_{0i}/4$ ($i = y, z$), and where $\bar{\Delta} = \omega - \omega_L$ with ω being the frequency of the probe field. The equation

above shows that the magneto-optical coupling to a dynamic magnetization, in the linear approximation, is equivalent to an effective ‘diamagnetic’ response. This becomes apparent if we consider the equation for $\delta\mathcal{E}^z$ where the magneto-optical contribution competes with the ordinary ferromagnetic resonance [$\sim \chi_{yy}(\omega)$] from the y -component of the fluctuating magnetic field.

2.2. Magneto-optical coupling mechanism

A possible origin for the effective diamagnetic contribution in (10) and (11) can be understood from a quantized optomagnonic Hamiltonian [15, 16]. For this purpose, we consider a spin $\mathbf{S} = \mathbf{S}\delta(\mathbf{r} - \mathbf{r}_0)$ coupled to the electric field through the magneto-optical coupling

$$\mathcal{H}_{\text{mo}} = -\frac{\varepsilon_0}{4} \int \delta\varepsilon_{ij} \mathcal{E}_i \mathcal{E}_j^* d^3r, \quad (12)$$

where $\delta\varepsilon_{ij} = if\epsilon_{ijk}S_k$ describes the inverse Faraday effect with $f = 2c\theta_F/(\sqrt{\varepsilon}\omega S)$ [15], where θ_F is the Faraday rotation angle, c is the velocity of light, ω is the frequency of the electromagnetic wave, and ε is the electric permittivity of the medium. In what follows, we take the electric field in the form of cavity standing waves along the x axis, $\mathcal{E}(x) = \sum_{\lambda=L,R} [\hbar\omega_c/(\varepsilon_0 V)]^{1/2} \sin(\pi n x_0/L_x) \mathbf{e}_\lambda a_\lambda$, where a_λ is the cavity photon annihilation operator, $\mathbf{e}_\lambda = (0, \lambda, i)/\sqrt{2}$ is the polarization vector for the circularly polarized wave with the left ($L = -1$) or right ($R = 1$) polarization λ , n is the cavity mode index, V is the volume of the cavity, L_x is the size of the cavity along the x direction, and x_0 denotes the position of the sample. We take the z -axis as a quantization axis for the spin \mathbf{S} , as shown in Fig. 2 (a), so that the magneto-optical coupling becomes

$$\mathcal{H}_{\text{mo}} = \hbar g_0 (a_L^\dagger a_L - a_R^\dagger a_R) (b + b^\dagger), \quad (13)$$

where $g_0 = c\theta_F\xi/\sqrt{2\varepsilon S}$ is the magnon-photon coupling parameter at the node where the electric field is at the maximum ($\xi \lesssim 1$ is a geometric factor). For μm sized yttrium iron garnet sample at the optical wavelength $\sim 1 \mu\text{m}$, we can estimate $\theta_F = 200^\circ \text{ cm}^{-1}$ [40, App. A], $\varepsilon \approx 5$ and $S = 10^{10}$, which gives $g_0 \approx 10^5 \text{ Hz}$ [15].

The interaction energy in (13) is the same as in optomechanical applications. In the rotating wave approximation (RWA), the total Hamiltonian can be written as

$$\mathcal{H} = -\hbar\Delta(a_1^\dagger a_1 + a_2^\dagger a_2) + \hbar\Omega_m b^\dagger b + i\hbar g_0 (a_2^\dagger a_1 - a_1^\dagger a_2) (b + b^\dagger) + i\hbar\sqrt{\kappa_{\text{ex}}}(\alpha a_1^\dagger - i\alpha^* a_1), \quad (14)$$

where α is the amplitude of the driving field, and we have transformed to the linearly polarized basis, $a_L = (a_1 - ia_2)/\sqrt{2}$ and $a_R = (a_1 + ia_2)/\sqrt{2}$. The last term in this expression is the external driving, which becomes time independent under the RWA [1]. Compared to the magneto-dipole interaction in (1), the optomechanical coupling in RWA leads to the detuning parameter $\Delta = \omega_L - \omega_c$ that may have an arbitrary sign depending on the ratio of the driving frequency, ω_L , to ω_c .

The interaction part of the Hamiltonian (14) can be linearized as follows:

$$a_2^\dagger a_1 - a_1^\dagger a_2 \approx \sqrt{n_2}(a_1 - a_1^\dagger) - \sqrt{n_1}(a_2 - a_2^\dagger), \quad (15)$$

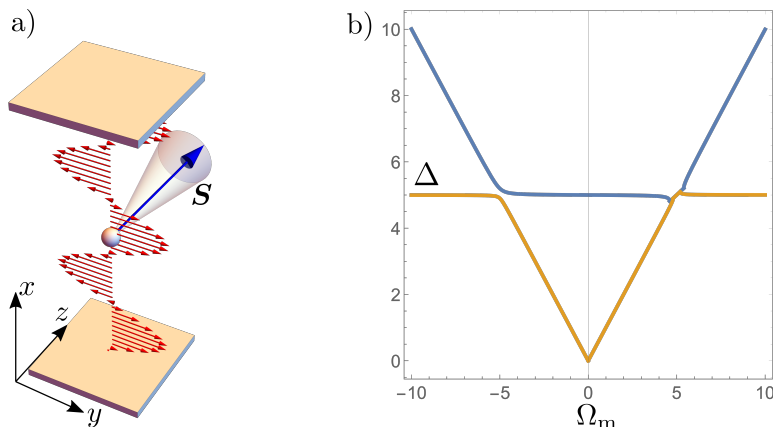


Figure 2. a) Experimental geometry for the magneto-optical mechanism of the mode attraction. b) Energy dispersion (18a, 18b) as a function of Ω_m .

where n_1 and n_2 denote the average numbers of cavity photons. The linearized Hamiltonian is written as

$$\begin{aligned} \mathcal{H}_{\text{lin}} = & -\hbar\Delta(a_1^\dagger a_1 + a_2^\dagger a_2) + \hbar\Omega_m b^\dagger b + i\hbar g_1(a_1 - a_1^\dagger)(b + b^\dagger) \\ & - i\hbar g_2(a_2 - a_2^\dagger)(b + b^\dagger) + i\hbar\sqrt{\kappa_{\text{ex}}}(\alpha a_1^\dagger - i\alpha^* a_1), \end{aligned} \quad (16)$$

where we have introduced renormalized coupling parameters $g_1 = g_0\sqrt{n_2}$ and $g_2 = g_0\sqrt{n_1}$. In a situation where the driving field is coupled only to the cavity photon of one polarization, we would normally expect $g_2 \gg g_1$.

The Heisenberg equations of motion for the Hamiltonian (16) can be written in the matrix form:

$$-i\partial_t \begin{pmatrix} a_1 \\ a_1^\dagger \\ a_2 \\ a_2^\dagger \\ b \\ b^\dagger \end{pmatrix} = \begin{pmatrix} \Delta & 0 & 0 & 0 & ig_1 & ig_1 \\ 0 & -\Delta & 0 & 0 & ig_1 & ig_1 \\ 0 & 0 & \Delta & 0 & -ig_2 & -ig_2 \\ 0 & 0 & 0 & -\Delta & -ig_2 & -ig_2 \\ -ig_1 & ig_1 & ig_2 & -ig_2 & -\Omega_m & 0 \\ ig_1 & -ig_1 & -ig_2 & ig_2 & 0 & \Omega_m \end{pmatrix} \begin{pmatrix} a_1 \\ a_1^\dagger \\ a_2 \\ a_2^\dagger \\ b \\ b^\dagger \end{pmatrix} - i \begin{pmatrix} \alpha \\ \alpha^* \\ 0 \\ 0 \\ 0 \\ 0 \end{pmatrix}, \quad (17)$$

which has a pair of trivial eigenvalues $\omega_0 = \pm\Delta$, and two pairs of hybridized eigenmodes

$$\omega^{(+)} = \pm\sqrt{\frac{\Delta^2 + \Omega_m^2}{2} + \sqrt{\frac{(\Delta^2 - \Omega_m^2)^2}{4} - 4(g_1^2 + g_2^2)\Delta\Omega_m}}, \quad (18a)$$

$$\omega^{(-)} = \pm\sqrt{\frac{\Delta^2 + \Omega_m^2}{2} - \sqrt{\frac{(\Delta^2 - \Omega_m^2)^2}{4} - 4(g_1^2 + g_2^2)\Delta\Omega_m}}. \quad (18b)$$

In accordance with [29], for $\Delta > 0$, $\omega^{(\pm)}$ demonstrate level attraction in the region where $(\Delta^2 - \Omega_m^2)^2 < 16(g_1^2 + g_2^2)\Delta\Omega_m$, which is related to the parametric instability in cavity optomechanics [1]. This region is bounded by the exceptional points, where the eigenmodes coalesce, and the matrix on the right-hand side of (17) is characterized by

the Jordan form:

$$\begin{pmatrix} -\Delta & 0 & 0 & 0 & 0 & 0 \\ 0 & \Delta & 0 & 0 & 0 & 0 \\ 0 & 0 & -\sqrt{\frac{\Omega_m^2 + \Delta^2}{2}} & 1 & 0 & 0 \\ 0 & 0 & 0 & -\sqrt{\frac{\Omega_m^2 + \Delta^2}{2}} & 0 & 0 \\ 0 & 0 & 0 & 0 & \sqrt{\frac{\Omega_m^2 + \Delta^2}{2}} & 1 \\ 0 & 0 & 0 & 0 & 0 & \sqrt{\frac{\Omega_m^2 + \Delta^2}{2}} \end{pmatrix}. \quad (19)$$

For $\Delta < 0$, in contrast, we have usual mode repulsion. Remarkably, the energy-level picture for the dispersion relations (18a, 18b) shown in Fig. 2 (b) becomes similar to that in Fig. 1 (b) for the three-oscillator model with inverted horizontal axis.

Solutions of equations of motion (17) for the cavity modes have the following form

$$a_1 = \frac{i\alpha}{\Delta} \frac{\Delta\Omega_m + 4g_2^2}{\Delta\Omega_m + 4(g_1^2 + g_2^2)}, \quad a_2 = \frac{4i\alpha g_1 g_2}{\Delta[\Delta\Omega_m + 4(g_1^2 + g_2^2)]}, \quad (20)$$

where we used real α for simplicity. If $g_1 \sim \sqrt{n_2}$ is nonzero, driving of a_1 excites also a_2 . In this situation, if we take into account the dissipation of the cavity mode, $\Delta \rightarrow \Delta + i\kappa_c$, the response in (20) has 2π -phase shift with respect to the drive due to the degeneracy of the cavity modes with different polarizations.

3. Aharonov-Casher effect

Here, we discuss another mechanism of mode attraction for a coupled magnon-photon dynamics inside a ferromagnetic insulator based on the Aharonov-Casher effect [37]. This effect is related to a dualism between the electrodynamics of electric charges in a magnetic field and that of charge-neutral magnetic dipoles in an electric field. When applied to magnon dynamics this leads, for example, to the Landau quantization of the magnon states under applied electric field gradient [41]. Since the diamagnetism of a conventional electron gas follows from Landau quantization of electron motion, by analogy, we expect that a sort of ‘diamagnetic’ response should also exist for magnons in the electric field. which, In turn, this provides us with a mechanism for the level attraction, as explained below.

For this purpose, we consider the following spin Hamiltonian for a small ferromagnetic specimen

$$\mathcal{H} = - \sum_{\langle ij \rangle} \left[\frac{J}{2} \left(S_i^{(-)} S_j^{(+)} e^{i\theta_{ij}} + S_i^{(+)} S_j^{(-)} e^{-i\theta_{ij}} \right) + J S_i^{(z)} S_j^{(z)} \right] - K \sum_i \left[S_i^{(z)} \right]^2, \quad (21)$$

where J is the ferromagnetic exchange constant, K is the anisotropy parameter, and the summation is over the nearest neighbouring sites limited by the size of the specimen. The first term contains a field phase associated with the cavity electric field. The phase factor is given by [41]

$$\theta_{ij}(t) = \frac{g\mu_B}{\hbar c^2} \int_{\mathbf{r}_i}^{\mathbf{r}_j} [\mathbf{E}(\mathbf{r}, t) \times \hat{\mathbf{z}}] \cdot d\ell, \quad (22)$$

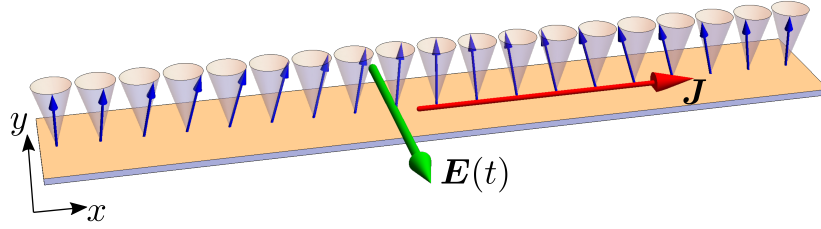


Figure 3. Schematic picture of a spin wave inside a small ferromagnetic specimen carrying spin current \mathbf{J} along the x direction interacting with the cavity electric field \mathbf{E} polarized along the y axis. The electric field is supposed to be homogeneous on the specimen's length scale.

where the integration is taken along the path connecting i th and j th sites, and z plays the role of a spin quantization axis.

If we suppose that the characteristic wavelength of the electric field is much larger than the sample size, then the interaction part in the Hamiltonian (21) can be written in the form $-\mathbf{E} \cdot \mathbf{J}$, where $\mathbf{J} = [ig\mu_B J / (2\hbar c^2)] \sum_{\langle ij \rangle} (S_i^{(-)} S_j^{(+)} - S_i^{(+)} S_j^{(-)}) [\hat{\mathbf{z}} \times \mathbf{r}_{ij}]$ is the spin current in the sample (see Fig. 3). By quantizing the spin operators, $S_i^{(+)} = \sqrt{2S} b_i$, $S_i^{(-)} = \sqrt{2S} b_i^\dagger$, and choosing the electric field in the form of a linearly polarized cavity standing wave along the x direction, $E_y(x) = [\hbar\omega_c / (\varepsilon_0 V)]^{1/2} \sin(\pi n x / L_x) (a + a^\dagger)$, the interaction energy can be written as $-\hbar \sum_{\mathbf{k}} g_{\mathbf{k}} b_{\mathbf{k}}^\dagger b_{\mathbf{k}} (a + a^\dagger)$, where the interaction constant $g_{\mathbf{k}} = -[2g\mu_B J S / (\hbar^2 c^2)] [\hbar\omega_c / (\varepsilon_0 V)]^{1/2} \sin(\pi n x_0 / L_x) \sum_{\delta} \sin(\mathbf{k} \cdot \delta) (\hat{\mathbf{z}} \times \delta)_y$ generally depends on the position of the sample x_0 with respect to the electric field.

If the sample is populated into a state with $n_{\mathbf{k}_0} \gg n_{-\mathbf{k}_0}$ for some \mathbf{k}_0 , where $n_{\mathbf{k}} = \langle b_{\mathbf{k}}^\dagger b_{\mathbf{k}} \rangle$ is the magnon number, and magnon states with different \mathbf{k} are well separated, we can consider a simplified model

$$\mathcal{H} = \hbar\omega_c a^\dagger a + \hbar\Omega_{\mathbf{k}_0} b_{\mathbf{k}_0}^\dagger b_{\mathbf{k}_0} - \hbar g_{\mathbf{k}_0} b_{\mathbf{k}_0}^\dagger b_{\mathbf{k}_0} (a + a^\dagger) + \mathcal{H}_{\text{dr}}^{(\text{m})}, \quad (23)$$

where we added the driving term $\mathcal{H}_{\text{dr}}^{(\text{m})} = i\hbar\sqrt{\kappa_{\text{ex}}}\beta_{\mathbf{k}_0}^{(\text{in})} b_{\mathbf{k}_0} \exp(-i\omega t) + \text{H.c.}$, with the amplitude of the driving field $\beta_{\mathbf{k}_0}^{(\text{in})}$. The Hamiltonian (23) can be considered as dual to the model with magneto-optical interactions in equations (13, 14). It can be interpreted in terms of the pressure force created by the magnon flow with finite \mathbf{k}_0 on the cavity photon oscillator, with the position operator proportional to $a + a^\dagger$.

Similar to optomagnonic Hamiltonian (14), equation (23) can be transformed to the time-independent frame by applying the unitary transformation to the magnon operators, $b_{\mathbf{k}_0} \rightarrow \exp(b_{\mathbf{k}_0}^\dagger b_{\mathbf{k}_0} t) b_{\mathbf{k}_0}$ [1]. In this representation, the magnon frequency is replaced by the magnon detuning parameter, $\Omega_{\mathbf{k}_0} \rightarrow -\tilde{\Delta}$, where $\tilde{\Delta} = \omega - \Omega_{\mathbf{k}_0}$, with which we can reach the attraction regime in the region $(\tilde{\Delta} - \omega_c)^2 < 4g_{\mathbf{k}_0}^2 n_{\mathbf{k}_0}$. We note that, in contrast to optomagnonic case, the single magnon coupling constant is small compared to $\Omega_{\mathbf{k}_0}$. For realistic parameters, $J = 100$ K, $\omega_c = 10^{12}$ s $^{-1}$, and $S = 1$, we estimate $g_{\mathbf{k}_0} = 10^{-4}$ s $^{-1}$, which means that the effect is difficult to realize experimentally. However, we believe that it can be relevant to ultrafast magnetization

dynamics in metamaterials with $S \gg 1$, and can provide an experimental evidence for the spin current electrodynamics proposed in [37].

4. Summary

We considered several mechanisms of mode attraction for a coupled magnon-photon system inside a microwave cavity. Using the Maxwell's equations of continuous media, we demonstrated how the level attraction can be described in terms of response functions of the medium. In particular, we derived the effective permittivity for the inverse Faraday effect, and showed that it can be interpreted as an effective diamagnetic effect in the equations of motion for the electromagnetic fields inside the cavity. This approach has been supported by the quantum picture based on the optomagnonic Hamiltonian [15, 16], which has reasonable parameter values for experimental demonstration of the effect.

Also, we discussed another mechanism, which is based on the electro-dipole effect of the magnon spin current [42]. In the context of level attraction, this mechanism can be considered as dual to optomagnonic approach because it requires driving of the magnon mode with finite wave vector. This effect is relativistically small compared to the magneto-optical mechanism.

Acknowledgments

The authors thank Can-Min Hu and Michael Harder for stimulating discussions. I.P. is supported by the Ministry of Education and Science of the Russian Federation, Grant No. MK-1731.2018.2, and by the Russian Foundation for Basic Research (RFBR), Grant No. 18-32-00769. R.L.S. acknowledges the support of the Natural Sciences and Engineering Research Council of Canada (NSERC) RGPIN 05011-18. The work of R. Macêdo is supported by the Leverhulme Trust.

Appendix A. Resonant frequencies for the three-oscillator model

In order to derive the Hamiltonian (1), we consider the magnetization $\mathbf{M}(t)$ in the static magnetic field \mathbf{H}_0 along the z -direction interacting with the microwave field $\mathbf{h}(t)$ [see Fig. 1 (a)]. By splitting the magnetization into static and dynamic parts, $\mathbf{M} = [M_s - m^2/(2M_s)]\hat{z} + \mathbf{m}(t)$, where M_s is the saturation magnetization and $\mathbf{m}(t)$ is the transverse dynamical component, the magnetic part of the energy, $\mathcal{H}_m = -\mathbf{M} \cdot \mathbf{H}_0 - \mathbf{h} \cdot \mathbf{M}$, in the linear approximation, becomes

$$\mathcal{H}_m = \hbar\Omega_m b^\dagger b - \frac{M_s}{\sqrt{2}} (h^{(-)}b + h^{(+)}b^\dagger), \quad (\text{A.1})$$

where $\Omega_m = \hbar^{-1}M_s H_0$, $h^{(\pm)} = h_x \pm ih_y$, and the circular components of \mathbf{m} are expressed via the Holstein-Primakoff boson operators, $m^{(+)} = \sqrt{2}M_s b$ and $m^{(-)} = \sqrt{2}M_s b^\dagger$. We

take the resonant cavity mode in the form of a plane wave along the z -direction, so that the magnetic field is quantized as follows:

$$\mathbf{h}(z, t) = i \sum_{\lambda} \left(\frac{\hbar \omega_c}{\mu_0 V} \right)^{\frac{1}{2}} \cos \left(\frac{\pi N_c z}{L_z} \right) \left[a_{\lambda} (\hat{\mathbf{z}} \times \mathbf{e}_{\lambda}) - a_{\lambda}^{\dagger} (\hat{\mathbf{z}} \times \mathbf{e}_{\lambda}^*) \right], \quad (\text{A.2})$$

where ω_c and N_c denote the frequency and the index of the cavity mode, V is the volume of the cavity, L_z is the size of the cavity along the z -axis, and a_{λ} (a_{λ}^{\dagger}) is the photon creation (annihilation) operator in the helicity basis $\mathbf{e}_{\lambda} = (\lambda, i, 0)/\sqrt{2}$ with $\lambda = 1$ (-1) for the right (left) polarized wave. Using this quantization of the magnetic field in (A.1), and adding the electromagnetic energy of cavity photons, we obtain the Hamiltonian (1) with $g_0 = (\omega_c M_s^2 / \hbar \mu_0 V)^{1/2}$ if the sample is at the position of maximum magnetic field.

The Heisenberg equations of motion for the Hamiltonian (1) with the driving have the following form:

$$-i\dot{a}_R = -\omega_c a_R - g_0 b^{\dagger} - i\sqrt{\kappa_{\text{ex}}} \alpha_{\text{in}} e^{-i\omega t}, \quad (\text{A.3})$$

$$-i\dot{b}^{\dagger} = \Omega_m b^{\dagger} + g_0 a_R + g_0 a_L^{\dagger}, \quad (\text{A.4})$$

$$-i\dot{a}_L^{\dagger} = \omega_c a_L^{\dagger} + g_0 b^{\dagger}. \quad (\text{A.5})$$

The stationary response of the system to the driving at frequency ω can be found from the algebraic system of equations for the field amplitudes

$$\begin{pmatrix} \omega - \omega_c & -g_0 & 0 \\ g_0 & \omega + \Omega_m & g_0 \\ 0 & g_0 & \omega + \omega_c \end{pmatrix} \begin{pmatrix} a_R \\ b^{\dagger} \\ a_L^{\dagger} \end{pmatrix} = i\sqrt{\kappa_{\text{ex}}} \begin{pmatrix} \alpha_{\text{in}} \\ 0 \\ 0 \end{pmatrix}, \quad (\text{A.6})$$

which has the following solutions

$$a_R = \frac{i\sqrt{\kappa_{\text{ex}}} \alpha_{\text{in}} [(\omega + \omega_c)(\omega + \Omega_m) - g_0^2]}{(\omega^2 - \omega_c^2)(\omega + \Omega_m) + 2g_0^2 \omega_c}, \quad (\text{A.7})$$

$$b^{\dagger} = \frac{i\sqrt{\kappa_{\text{ex}}} \alpha_{\text{in}} g_0 (\omega + \omega_c)}{(\omega^2 - \omega_c^2)(\omega + \Omega_m) + 2g_0^2 \omega_c}, \quad (\text{A.8})$$

$$a_L^{\dagger} = \frac{i\sqrt{\kappa_{\text{ex}}} \alpha_{\text{in}} g_0^2}{(\omega^2 - \omega_c^2)(\omega + \Omega_m) + 2g_0^2 \omega_c}. \quad (\text{A.9})$$

The resonant frequencies can be obtained from the determinant of the matrix on the left hand side of equation (A.6), $(\omega^2 - \omega_c^2)(\omega + \Omega_m) + 2g_0^2 \omega_c = 0$. The solutions have the form

$$\omega_0 = -\frac{1}{3} \left[\Omega_m + (A - iC)^{\frac{1}{3}} + (A + iC)^{\frac{1}{3}} \right], \quad (\text{A.10})$$

$$\omega_1 = -\frac{1}{3} \left[\Omega_m - e^{i\pi/3} (A - iC)^{\frac{1}{3}} - e^{-i\pi/3} (A + iC)^{\frac{1}{3}} \right], \quad (\text{A.11})$$

$$\omega_2 = -\frac{1}{3} \left[\Omega_m - e^{-i\pi/3} (A - iC)^{\frac{1}{3}} - e^{i\pi/3} (A + iC)^{\frac{1}{3}} \right], \quad (\text{A.12})$$

where $A = \Omega_m^3 - 9\Omega_m \omega_c^2 + 27g_0^2 \omega_c$ and $B = \Omega_m^2 + 3\omega_c^2$, and $C = \sqrt{B^3 - A^2}$. The frequencies are real in the region where $B^3 \geq A^2$. Otherwise, ω_1 and ω_2 become complex. In the limit $g_0 = 0$, we have $\omega_0 = -\Omega_m$, $\omega_1 = -\omega_c$, and $\omega_2 = \omega_c$.

Appendix B. The effective permittivity for the inverse Faraday effect

In order to derive the effective response for the inverse Faraday effect, we consider the electric displacement field

$$\delta D_i(t) = i\varepsilon_0 f \epsilon_{ijx} m_x(t) E_j(t). \quad (\text{B.1})$$

In the Fourier space, this expression can be written as

$$D_i(\omega) = i\varepsilon_0 f \epsilon_{ijx} \int_{-\infty}^{\infty} \frac{d\omega'}{2\pi} \chi_{xx}(\omega') H_x^{\text{eff}}(\omega') E_j(\omega - \omega'), \quad (\text{B.2})$$

where the magnetization dynamics in the effective field is taken into account through the ferromagnetic susceptibility, $m_x(\omega) = \chi_{xx}(\omega) H_x^{\text{eff}}(\omega)$, and the Fourier components of the fields are determined as follows $F(\omega) = \int_{-\infty}^{\infty} dt e^{i\omega t} F(t)$. The Fourier component of the effective field is given by

$$\mathbf{H}^{\text{eff}} = \frac{i\varepsilon_0 f}{4} \int_{-\infty}^{\infty} \frac{d\omega'}{2\pi} \mathcal{E}(\omega') \times \mathcal{E}^*(\omega - \omega'), \quad (\text{B.3})$$

which gives after substitution into (B.2)

$$\begin{aligned} D_i(\omega) &= -\frac{\varepsilon_0^2 f^2}{8} \epsilon_{ijx} \epsilon_{klx} \int_{-\infty}^{\infty} \frac{d\omega'}{2\pi} \int_{-\infty}^{\infty} \frac{d\omega''}{2\pi} \chi_{xx}(\omega') \mathcal{E}_k(\omega'') \mathcal{E}_l(\omega' - \omega'') \\ &\times [\mathcal{E}_j(\omega - \omega') + \mathcal{E}_j^*(\omega - \omega')]. \end{aligned} \quad (\text{B.4})$$

We imply that the electric field is driven by the external field $\mathbf{E}_0(t) = [\mathcal{E}_0 \exp(-i\omega_L t) + \mathcal{E}_0^* \exp(i\omega_L t)]/2$, and expand (B.4) up to the linear order in the fluctuating field, $\mathbf{E} = \mathbf{E}_0 + \delta\mathbf{E}$, which gives after some algebra

$$\begin{aligned} \delta D_i(\omega) &= -\frac{\varepsilon_0^2 f^2}{8} \epsilon_{ijx} \left\{ \chi_{xx}(0) (\mathcal{E}_0 \times \mathcal{E}_0^*)_x [\delta\mathcal{E}_j(\omega) + \delta\mathcal{E}_j^*(\omega)] \right. \\ &+ \chi_{xx}(\omega - \omega_L) \mathcal{E}_{0j} [\mathcal{E}_{0z}^* \delta\mathcal{E}_y(\omega) - \mathcal{E}_{0y}^* \delta\mathcal{E}_z(\omega)] \\ &+ \chi_{xx}(\omega + \omega_L) \mathcal{E}_{0j}^* [\mathcal{E}_{0y} \delta\mathcal{E}_z^*(\omega) - \mathcal{E}_{0z} \delta\mathcal{E}_y^*(\omega)] \\ &+ \chi_{xx}(\omega - \omega_L) \mathcal{E}_{0j} [\mathcal{E}_{0y} \delta\mathcal{E}_z^*(\omega - 2\omega_L) - \mathcal{E}_{0z} \delta\mathcal{E}_y^*(\omega - 2\omega_L)] \\ &\left. + \chi_{xx}(\omega + \omega_L) \mathcal{E}_{0j}^* [\mathcal{E}_{0z}^* \delta\mathcal{E}_y(\omega + 2\omega_L) - \mathcal{E}_{0y}^* \delta\mathcal{E}_z(\omega + 2\omega_L)] \right\}. \end{aligned} \quad (\text{B.5})$$

Neglecting the last terms with $\omega \pm 2\omega_L$ and the first term, which corresponds to the static component of the effective field, we obtain equation (10).

- [1] M. Aspelmeyer, T. J. Kippenberg, and F. Marquardt. Cavity optomechanics. *Rev. Mod. Phys.*, 86:1391–1452, 2014.
- [2] M. Eichenfield, J. Chan, R. M. Camacho, K. J. Vahala, and O. Painter. Optomechanical crystals. *Nature*, 462(7269):78, 2009.
- [3] M. Harder and C.-M. Hu. Cavity spintronics: An early review of recent progress in the study of magnon-photon level repulsion. *Solid State Physics*, 69:47–121, 2018.
- [4] Y. Tabuchi, S. Ishino, T. Ishikawa, R. Yamazaki, K. Usami, and Y. Nakamura. Hybridizing ferromagnetic magnons and microwave photons in the quantum limit. *Phys. Rev. Lett.*, 113:083603, 2014.
- [5] X. Zhang, C.-L. Zou, L. Jiang, and H. X. Tang. Strongly coupled magnons and cavity microwave photons. *Phys. Rev. Lett.*, 113:156401, 2014.

- [6] L. Bai, M. Harder, Y. P. Chen, X. Fan, J. Q. Xiao, and C.-M. Hu. Spin pumping in electro-dynamically coupled magnon-photon systems. *Phys. Rev. Lett.*, 114:227201, 2015.
- [7] Y. Cao, P. Yan, H. Huebl, S. T. B. Goennenwein, and G. E. W. Bauer. Exchange magnon-polaritons in microwave cavities. *Phys. Rev. B*, 91:094423, 2015.
- [8] B. M. Yao, Y. S. Gui, Y. Xiao, H. Guo, X. S. Chen, W. Lu, C. L. Chien, and C.-M. Hu. Theory and experiment on cavity magnon-polariton in the one-dimensional configuration. *Phys. Rev. B*, 92:184407, 2015.
- [9] D. Zhang, X.-M. Wang, T.-F. Li, X.-Q. Luo, W. Wu, F. Nori, and J. Q. You. Cavity quantum electrodynamics with ferromagnetic magnons in a small yttrium-iron-garnet sphere. *Quantum Information*, 1:15014, 2015.
- [10] M. Harder, P. Hyde, L. Bai, C. Match, and C.-M. Hu. Spin dynamical phase and antiresonance in a strongly coupled magnon-photon system. *Phys. Rev. B*, 94:054403, 2016.
- [11] H. Maier-Flaig, M. Harder, R. Gross, H. Huebl, and S. T. B. Goennenwein. Spin pumping in strongly coupled magnon-photon systems. *Phys. Rev. B*, 94:054433, 2016.
- [12] B. Yao, Y. S. Gui, J. W. Rao, S. Kaur, X. S. Chen, W. Lu, Y. Xiao, H. Guo, K.-P. Marzlin, and C.-M. Hu. Cooperative polariton dynamics in feedback-coupled cavities. *Nature communications*, 8(1):1437, 2017.
- [13] X. Zhang, C.-L. Zou, L. Jiang, and H. X. Tang. Cavity magnomechanics. *Science Advances*, 2(3):e1501286, 2016.
- [14] A. Osada, R. Hisatomi, A. Noguchi, Y. Tabuchi, R. Yamazaki, K. Usami, M. Sadgrove, R. Yalla, M. Nomura, and Y. Nakamura. Cavity optomagnonics with spin-orbit coupled photons. *Phys. Rev. Lett.*, 116:223601, 2016.
- [15] S. Viola Kusminskiy, H. X. Tang, and F. Marquardt. Coupled spin-light dynamics in cavity optomagnonics. *Phys. Rev. A*, 94:033821, 2016.
- [16] T. Liu, X. Zhang, H. X. Tang, and M. E. Flatté. Optomagnonics in magnetic solids. *Phys. Rev. B*, 94:060405, 2016.
- [17] S. Sharma, Y. M. Blanter, and G. E. W. Bauer. Optical cooling of magnons. *Phys. Rev. Lett.*, 121:087205, 2018.
- [18] C.-H. Dong, Z. Shen, C.-L. Zou, Y.-L. Zhang, W. Fu, and G.-C. Guo. Brillouin-scattering-induced transparency and non-reciprocal light storage. *Nature communications*, 6:6193, 2015.
- [19] X. Zhang, N. Zhu, C.-L. Zou, and H. X. Tang. Optomagnonic whispering gallery microresonators. *Phys. Rev. Lett.*, 117:123605, 2016.
- [20] S. Sharma, Y. M. Blanter, and Gerrit E. W. Bauer. Light scattering by magnons in whispering gallery mode cavities. *Phys. Rev. B*, 96:094412, 2017.
- [21] J. Graf, H. Pfeifer, F. Marquardt, and S. Viola Kusminskiy. Cavity optomagnonics with magnetic textures: Coupling a magnetic vortex to light. *Phys. Rev. B*, 98:241406, Dec 2018.
- [22] I. Proskurin, A. S. Ovchinnikov, J. Kishine, and R. L. Stamps. Cavity optomechanics of topological spin textures in magnetic insulators. *Phys. Rev. B*, 98:220411, 2018.
- [23] N. J. Lambert, J. A. Haigh, S. Langenfeld, A. C. Doherty, and A. J. Ferguson. Cavity-mediated coherent coupling of magnetic moments. *Phys. Rev. A*, 93:021803, 2016.
- [24] B. Zare Rameshti and G. E. W. Bauer. Indirect coupling of magnons by cavity photons. *Phys. Rev. B*, 97:014419, 2018.
- [25] L. Bai, M. Harder, P. Hyde, Z. Zhang, C.-M. Hu, Y. P. Chen, and J. Q. Xiao. Cavity mediated manipulation of distant spin currents using a cavity-magnon-polariton. *Phys. Rev. Lett.*, 118:217201, May 2017.
- [26] Øyvind Johansen and Arne Brataas. Nonlocal coupling between antiferromagnets and ferromagnets in cavities. *Phys. Rev. Lett.*, 121:087204, 2018.
- [27] M. Harder, Y. Yang, B. M. Yao, C. H. Yu, J. W. Rao, Y. S. Gui, R. L. Stamps, and C.-M. Hu. Level attraction due to dissipative magnon-photon coupling. *Phys. Rev. Lett.*, 121:137203, 2018.
- [28] Y. Yang, J.W. Rao, Y.S. Gui, B.M. Yao, W. Lu, and C.-M. Hu. Control of the magnon-photon level attraction in a planar cavity. *Phys. Rev. Applied*, 11:054023, 2019.

- [29] N. R. Bernier, L. D. Tóth, A. K. Feofanov, and T. J. Kippenberg. Level attraction in a microwave optomechanical circuit. *Phys. Rev. A*, 98:023841, 2018.
- [30] A. P. Seyranian, O. N. Kirillov, and A. A. Mailybaev. Coupling of eigenvalues of complex matrices at diabolic and exceptional points. *J. Phys. A: Math. Gen.*, 38(8):1723–1740, 2005.
- [31] W. D. Heiss. The physics of exceptional points. *J. Phys. A: Math. Theor.*, 45(44):444016, 2012.
- [32] V. L. Grigoryan, K. Shen, and K. Xia. Synchronized spin-photon coupling in a microwave cavity. *Phys. Rev. B*, 98:024406, 2018.
- [33] I. Boventer, C. Dörflinger, T. Wolz, R. Macêdo, R. Lebrun, M. Kläui, and M. Weides. Control of the coupling strength and the linewidth of a cavity-magnon polariton. *arXiv:1904.00393*, 2019.
- [34] Isabella Boventer, Mathias Kläui, Rair Macêdo, and Martin Weides. Steering between level repulsion and attraction: Beyond single-tone driven cavity magnon-polaritons. *arXiv*, page 1908.05439, 2019.
- [35] B. Zare Rameshti, Y. Cao, and G. E. W. Bauer. Magnetic spheres in microwave cavities. *Phys. Rev. B*, 91:214430, Jun 2015.
- [36] A. I. Akhiezer, V. G. Bar'yakhtar, and S. V. Peletminskii. *Spin waves*. North-Holland Publishing Company Amsterdam, 1968.
- [37] Y. Aharonov and A. Casher. Topological quantum effects for neutral particles. *Phys. Rev. Lett.*, 53:319–321, 1984.
- [38] J. D. Jackson. *Classical Electrodynamics, 3rd ed.* John Wiley & Sons, New York, 1998.
- [39] L. D. Landau, J. S. Bell, M. J. Kearsley, L. P. Pitaevskii, E. M. Lifshitz, and J. B. Sykes. *Electrodynamics of continuous media*, volume 8. Elsevier, 2013.
- [40] D. D. Stancil. *Theory of magnetostatic waves*. Springer Science & Business Media, 2012.
- [41] K. Nakata, J. Klinovaja, and D. Loss. Magnonic quantum hall effect and wiedemann-franz law. *Phys. Rev. B*, 95:125429, 2017.
- [42] F. Meier and D. Loss. Magnetization transport and quantized spin conductance. *Phys. Rev. Lett.*, 90:167204, 2003.